ARTICLE

Therapeutic Modalities of Squalenoyl Nanocomposites in Colon Cancer: An Ongoing Search for Improved Efficacy

Andrei Maksimenko,[†] Mouad Alami,[‡] Fatima Zouhiri,[†] Jean-Daniel Brion,[‡] Alain Pruvost,[§] Julie Mougin,[†] Abdallah Hamze,[‡] Tanguy Boissenot,[†] Olivier Provot,[‡] Didier Desmaële,[†] and Patrick Couvreur[†,*]

[†]Faculté de Pharmacie, Université Paris-Sud, Institut Galien Paris Sud, UMR CNRS 8612, 5 rue J.-B. Clément, Châtenay-Malabry, Paris, F-92296, France, [‡]Laboratoire de Chimie Thérapeutique, Equipe Labellisée Ligue Contre le Cancer, LabEx LERMIT, Faculté de Pharmacie, Université Paris-Sud, CNRS, BioCIS-UMR 8076, 5 rue J.-B. Clément, Châtenay-Malabry, Paris, F-92296, France, and [§]Laboratoire d'Etude du Métabolisme des Médicaments, iBiTecS, SPI, CEA, Gif sur Yvette, Paris F-91191, France

ABSTRACT Drug delivery of combined cytotoxic and antivascular chemotherapies in multidrug nanoassemblies may represent an attractive way to improve the treatment of experimental cancers. Here we made the proof of concept of this approach on the experimental LS174-T human colon carcinoma xenograft nude mice model. Briefly, we have nanoprecipitated the anticancer compound gemcitabine conjugated with squalene (SQ-gem) together with isocombretastatin A-4 (isoCA-4), a new isomer of the antivascular combretastatin A-4 (CA-4). It was found that these molecules spontaneously self-assembled as stable nanoparticles (SQ-gem/isoCA-4 NAs) of *ca.* 142 nm in a surfactant-free aqueous solution. Cell culture viability tests and apoptosis assays showed that SQ-gem/isoCA-4 NAs displayed comparable antiproliferative and cytotoxic effects than those of the native gemcitabine or the mixtures of free gemcitabine with isoCA-4. Surprisingly, it was observed by confocal microscopy that the nanocomposites made of SQ-gem/isoCA-4 distributed intracellularly as intact nanoparticles whereas the SQ-gem nanoparticles remained localized onto the cell membrane. When used to deliver these combined chemotherapeutics to human colon cancer model, SQ-gem/isoCA-4 nanocomposites induced complete tumor regression (by 93%) and were found superior to all the other treatments, whereas the overall tolerance was better than the free drug treatments. This approach could be applied to other pairs of squalenoylated nanoassemblies with other non-water-soluble drugs, thus broadening the application of the "squalenoylation" concept in oncology.

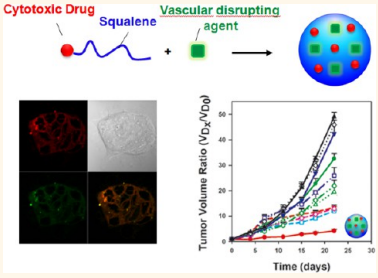

KEYWORDS: nanomedicine · chemotherapy · gemcitabine · squalene · isoCA-4 combretastatin isomer · colon cancer

Progression of cancer diseases are generally characterized by mechanisms involving both tumor neovascularization and cancer cell proliferation.[1−3] Indeed, in addition to its own proliferation process involving DNA replication, tubulin polymerization as well as apoptosis inhibition, tumor is also under the dependence of the development of neovasculature for providing nutriments and oxygen.[3−5] Therefore, the treatment of neoplastic diseases such as the colorectal cancer is often inefficient when using a single anticancer drug, either antimitotic or antiangiogenic. In addition, a single treatment may allow the easier emergence of resistances.[6,7] This is the reason why it is believed that the combination of antivascular drugs together with cytotoxic agents may significantly improve anticancer efficacy.[8,9] The original rationale for such combination is to destroy two separate components of tumors: endothelial and cancer cells.[10] However, when administrated as a free drug, antivascular compounds have long pharmacokinetic blood profiles, which induces shut down of tumor neovasculature, thus preventing further access to the tumor of cytotoxic agent, and suppression of tumor vascular formation may result in overexpression of hypoxia-factor-1a, which induces tumor metastasis and drug resistance.[10] Delivering an antivascular agent together with a cytotoxic drug as one nanoparticle may overcome these obstacles.[11,12] Coadministration of antivascular agents with cytotoxic drugs would simultaneously destroy two interdependent cell populations, yielding maximal benefit. However, one major challenge in engineering multifunctional nanoparticles is maintaining the simplicity in design to ensure future scale-up while incorporating the desired functionalities, especially the ability to simultaneously deliver distinct drugs. A logical approach would be

* Address correspondence to patrick.couvreur@u-psud.fr.

Received for review June 5, 2013 and accepted February 20, 2014.

Published online February 20, 2014
10.1021/nn500517a

to develop systems where a minimum number of components can achieve the cumulative desired pharmacological effect. With this aim, we have constructed unique multifunctional nanoassemblies composed of both vasculature disruptor isoCA-4, a new nonisomerizable isomer of combretastatin A-4, and anticancer drug gemcitabine (gem) conjugated with natural lipid squalene (SQ-gem bioconjugate).

Colorectal cancer is one of the leading cancer deaths worldwide associated with angiogenesis, thereby significantly affecting patient survival.[13,14] In this study, the human umbilical vein endothelial cells (HUVECs) involved in the tumor vessel formation and invasive LS174-T human colon carcinoma were chosen as the cell models. The major obstacle in the treatment of colon cancer LS174-T cells (*in vitro* and *in vivo*) is, indeed, the low chemosensitivity of this cell line to anticancer drugs. LS174-T cell grows invasively inward and recruits its vessels from the nude rat host.[15] The overall tumor vascular pattern is unorganized, suggesting limited control of new vessel formation. Furthermore, LS174-T colon adenocarcinoma cell adhesion involves glycolipids, glycoproteins, and integrins to bind stimulated HUVECs and induces upregulated endocytosis of E-selectin in endothelial cells attached with tumor cells.[16] In this regard, a multifunctional system composed of both antivascular agent and cytotoxic drug could destroy the two interdependent cell populations (*i.e.*, HUVECs and human colonic adenocarcinoma cell line LS174-T), inducing tumor suppression and providing insight toward the development of novel therapeutics to combat the spread of cancer.

Gemcitabine is a nucleoside analogue, active against various solid tumors and prescribed as a first intention for the treatment of pancreatic cancer.[17] Gemcitabine hydrochloride has been approved also in Japan for use in non-small-cell lung cancer and biliary tract cancer, and has been approved overseas for use in breast cancer, urinary bladder cancer, ovarian cancer, and cervical cancer. In preclinical studies, gemcitabine was shown to exert antitumor activity but at a high i.p. dose of 320 mg/kg in a subcutaneously grafted LS174-T tumor model.[18] However, after administration, this molecule undergoes a rapid deamination extra- and intracellularly to the biologically inactive metabolite 2,2-difluorodeoxyuridine (dFdU). In addition, the intracellular penetration of gemcitabine is strongly dependent on the nucleoside transporter hENT1, whose down regulation leads to resistance to the treatment.[19,20] Therefore, we have previously shown that the bioconjugation of gemcitabine with the natural and biocompatible lipid squalene induced the spontaneous formation of nanoparticles that were able to overcome the above-mentioned limitations of gemcitabine.[21] Indeed, gemcitabine-squalene (SQ-gem) nanoparticles were found to display improved anticancer activity, comparatively to gemcitabine free (gem) on various murine and human experimental cancer models.[22−24] This improved anticancer efficacy was attributed to a better pharmacokinetic and biodistribution,[25] as well as to an improved intracellular penetration, independent of the nucleoside transporter.[26]

On the other hand, isoCA-4 is a promising antivascular compound which has, however, never been tested *in vivo* because of its dramatic insolubility in water media.[27,28] isoCA-4 was chosen because of its chemical stability in contrast to the *Z*-natural stilbene CA-4. Indeed, this latter is prone to double-bond isomerization during storage and administration. The *E*-isomer displays dramatically reduced inhibition of cancer cell growth and tubulin assembly.[29]

We describe here a very easy procedure to design unique multifunctional nanocomposite system, made of both SQ-gem bioconjugate and antivascular isoCA-4 (SQ-gem/isoCA-4 NAs). The SQ-gem/isoCA-4 nanocomposites were first characterized by laser light scattering, cryogenic temperature transmission electron microscopy (Cryo-TEM) and drug release experiments. Their intracellular distribution and *in vitro* anticancer activity were tested on cancer cell line LS174-T and on HUVECs. The antitumor efficacy of the SQ-gem/isoCA-4 NAs has been further evaluated *in vivo* on the experimental LS174-T human colon carcinoma and found superior to all the other control treatments in terms of tumor growth inhibition, as also supported by immunohistological investigations.

RESULTS

Design and Characterization of Supramolecular Squalene-Based Nanocomposites. The new strategy we propose for multidrug therapy relies on the design of squalene-based nanocomposites made of the squalenoyl prodrug of a cytotoxic agent such as gemcitabine (for chemical synthesis of SQ-gem, see Supporting Information [SI]) and a new hydrophobic antivascular compound such as isoCA-4 (for chemical synthesis of isoCA-4 [Figure S1 in SI], see SI) (Figure 1). Prodrug-based nanoassembly suspensions (5 μmol mL^{-1}), suitable for intravenous infusion, were prepared by nanoprecipitation from an ethanolic solution as described in the Materials and Methods and in the SI. For comparison, squalenic acid nanoparticles loaded with isoCA-4 (SQCOOH/isoCA-4 NAs) were also prepared in similar conditions (see the Materials and Methods and SI). Because of the amphiphilic nature of the gemcitabine-squalene bioconjugate and the hydrophobic nature of the new antivascular agent isoCA-4, these molecules spontaneously self-assembled in aqueous solution to form stable nanocomposites (Table 1). By modifying the ratio of SQ-gem and isoCA-4 in the squalene-based nanocomposites, it was possible to select the optimal suspension containing nanoassemblies of 142-nm mean diameter with narrow particle size distribution

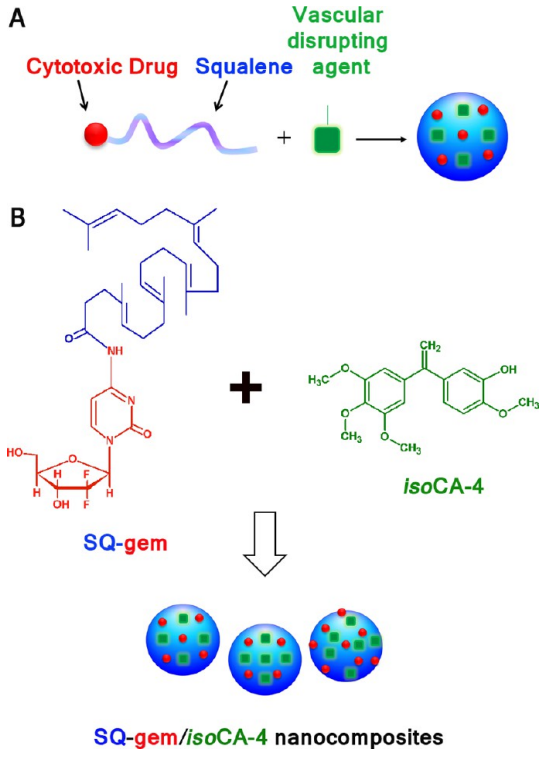

Figure 1. Design of squalene-based nanocomposites. (A) Strategy to achieve well-defined nanoassemblies for multidrug therapy. (B) Nanoprecipitation of the nanoassemblies composed of both SQ-gem bioconjugate and antiangiogenic compound isoCA-4.

(PSD < 0.1, as measured by quasielastic light scattering) (Table S1 in SI) and excellent colloidal stability for up to three months at 4 °C (Figure S2 in SI). For translation to clinic, we have also tested the stability of the SQ-gem/isoCA-4 NAs upon dilution (up to 50 000 times). The presence of the nanoassemblies was quite clearly detected in all the diluted suspensions (Table S3 in SI), and the size was found not to be influenced by dilution. The surface charge of the SQ-gem/isoCA-4 nanoassemblies ranged from −16 to −19 mV (Table 1), indicating that they were electrostatically stabilized. The size, size distribution, and zeta (ζ) potential of the NAs were reproducible, with three independent preparations giving nearly identical results for each sample. SQ-gem/isoCA-4 NAs were further characterized by cryoelectron microscopy (Figure 2B) and showed spherical shape and colloidal characteristics in good agreement with dynamic light scattering (DLS) data. Noteworthy, it was possible to distinguish again the supramolecular hexagonal phase organization of the SQ-gem NAs as previously described (Figure 2A, concentric circles),[30] whereas the absence of structure was noted with the new SQ-gem/isoCA-4 NAs (Figure 2B).

Importantly, our approach allowed nanocomposites with very high total drug contents of 60.1 wt % to be produced, containing both gemcitabine (27.3 wt %) and isoCA-4 (32.8 wt %) (Table 1). This is a significant improvement comparatively to common drug-loaded nanomedicines (*i.e.*, liposomes, nanoparticles, polymeric micelles *etc.*)[11,12] or even to squalenoyl nanoassemblies. The size and zeta (ζ) potential of SQ-gem NAs were nearly identical to the SQ-gem/isoCA-4 NAs (Table 1) but showed lower colloidal stability of less than one week, whereas SQ-gem/isoCA-4 NAs were stable during at least 90 days (Figure S2 in SI). The average diameter of SQCOOH/isoCA-4 (molar ratio 2:1, Table S2 in SI) NAs was 100 nm with a narrow PSD of 0.09, and a zeta (ζ) potential value of −39.3 mV (Table 1). Their colloidal stability was less than 4 days of storage at 4 °C (Figure S2 in SI).

Thus, the introduction of the isoCA-4 hydrophobic drug into squalenoyl gemcitabine NAs led to significant improvement of colloidal stability and drug payload. Incubation of nanoassemblies made of gemcitabine prodrugs in 90% (v/v) fetal calf serum (FCS) (for experimental details, see SI) resulted in a low release of free gemcitabine up to 24 h (Figure 2C,D). After 24 h of incubation, approximately 2.7 and 0.8% of the total gemcitabine content was, indeed, released in the presence of serum for SQ-gem NAs and SQ-gem/isoCA-4 NAs, respectively. On the contrary, isoCA-4 was observed to be released more rapidly than gemcitabine (26% of isoCA-4 was already released after 1 h incubation, whereas gemcitabine was not yet liberated at this time point); the sustained release of gemcitabine reached, however, 23% after 72 h. Interestingly, the release rate of gemcitabine from SQ-gem/isoCA-4 nanoassemblies was superior, comparatively to SQ-gem NAs (*i.e.*, 23% *versus* 11%, after 72 h incubation), whereas on the contrary, SQ-gem release was lower comparatively to SQ-gem nanoassemblies (*i.e.*, 4% *versus* 34% after 72 h incubation). But, the total pool of gemcitabine molecular species released (*i.e.*, gem+SQ-gem) from SQ-gem/isoCA-4 nanoassemblies remained lower, comparatively to SQ-gem nanoassemblies (*i.e.*, only 26% *versus* 45% after 72 h incubation). Clearly, the incorporation of lipophilic isoCA-4 into SQ-gem NAs stabilized the nanoassemblies and prolonged their half-life in biological medium.

***In Vitro* Cell Uptake and Antitumor Activity.** The influence of the insertion of isoCA-4 into NAs on their uptake by human colonic adenocarcinoma cell line LS174-T or HUVECs has been further investigated by confocal fluorescence microscopy (Figure 3A and Figure S3A in SI) and flow cytometry (Figure 3C,D and Figure S3C,D in SI).

In this view, we designed squalene-based nanocomposites labeled with two fluorescent cholesterol analogues, *i.e.*, CholEsteryl BODIPY 542/563 (BChol-red) and CholEsteryl BODIPY FL (BChol-green), to visualize NAs cellular capture and localization, the colocalization of the two fluorescent dyes being a strong indicator that NAs remained intact. Thus, the fluorescent nanocomposites, SQCOOH/isoCA-4/BChol-green/BChol-red, SQ-gem/BChol-green/BChol-red, and SQ-gem/isoCA-4/BChol-green/BChol-red, were prepared by nanoprecipitation as described in the Materials and Methods,

TABLE 1. Colloidal Characteristics of the Squalene-Based Nanocomposites

	size[a] (nm)	PSD[a]	ζ[b] (mV)	% gem[c] (wt %)	% isoCA-4[d] (wt %)	% (gem+isoCA-4)[e] (wt %)
SQ-gem NAs	133 ± 4	0.097	−15.1 ± 1.4	40.7	0	40.7
SQ-gem/isoCA-4 NAs	142 ± 6	0.086	−17.3 ± 1.2	27.3	32.8	60.1
SQCOOH/isoCA-4 NAs	100 ± 8	0.09	−39.3 ± 7.3	0	29.4	29.4

[a] Determined by DLS. [b] Zeta potential. [c] % gem = $MW_{gem}/MW_{nanocomposites}$. [d] % isoCA-4 = $MW_{isoCA-4}/MW_{nanocomposites}$. [e] % (isoCA-4+gem) = $MW_{(isoCA-4+gem)}/MW_{nanocomposites}$.

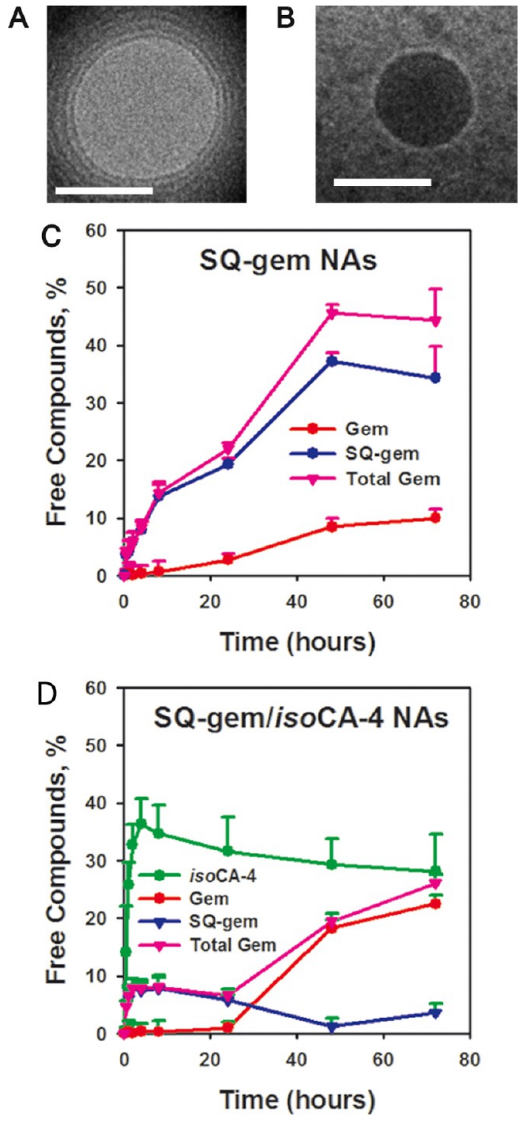

Figure 2. Characterization of squalene-based nanocomposites. Cryogenic transmission electron microscopy of SQ-gem (A) and SQ-gem/isoCA-4 (B) nanocomposites (scale bar, 100 nm). (C,D) Release of SQ-gem and gemcitabine from SQ-gem NAs (C) or SQ-gem, gemcitabine and isoCA-4 from SQ-gem/isoCA-4 NAs (D) at 37 °C in solution containing 90% (v/v) FCS. Released SQ-gem, gemcitabine or isoCA-4 was separated from squalenoyl gemcitabine nanoassemblies by ultracentrifugation (15000*g*; 30 min) and quantified in the supernatant using UPLC−MS/MS (for experimental details, see SI). Data represent the mean ± SD from triplicate independent experiments.

and their accumulation into cells was monitored at 515 and 560 nm in order to detect both fluorescent markers. A single mixture of the fluorescent cholesterol analogues was used as negative control.

With LS174-T human colon carcinoma cells, it was observed that after 4 h incubation, all types of NAs started to associate with cells; however, SQ-gem/BChol-green/BChol-red NAs reached a maximum at 8 h, while the intracellular fluorescence of SQCOOH/isoCA-4/BChol-green/BChol-red and SQ-gem/isoCA-4/BChol-green/BChol-red NAs continued to increase during the next 48 h incubation (Figure 3C,D). Thus, the presence of isoCA-4 into the SQ-gem/isoCA-4 NAs dramatically increased their interaction with cells. Moreover, as clearly shown in Figure 3A, SQ-gem NAs were found to localize only at the cell membrane without any intracellular accumulation of intact nanoparticles, which correlated with the previously published data.[26] To be noted that SQCOOH/isoCA-4 NAs localized at the cell membrane up to 8 h and penetrated inside the cells at 24 and 48 h. On the contrary, SQ-gem/isoCA-4/BChol-green/BChol-red NAs displayed intense intracellular fluorescence both in red and green channel with yellow colocalization, which indicated the presence of intact NAs into the cell cytoplasm (Figure 3A).

The same tendency was observed with HUVECs since SQ-gem/isoCA-4 NAs displayed a more important intracellular fluorescence than SQ-gem and SQCOOH/isoCA-4 NAs (Figure S3A in SI). Moreover, the cellular uptake of SQ-gem/isoCA-4 NAs in these cells was 2-times more important than in LS174-T cells (Figure 3C,D and Figure S3C,D in SI). The absence of any fluorescence signal after incubation of the control fluorescent cholesterol analogues mixture (BChol-green/BChol-red) with both cell lines got rid of possible fluorescent artifacts (Figure 3A and Figure S3A in SI). Noteworthy, the tested fluorescent nanocomposites demonstrated high stability since no fluorescence release could be observed under the same experimental conditions (Figure S6 in SI).

Then, the SQ-gem/isoCA-4 nanocomposites were evaluated for their cytotoxic activity *in vitro* toward the human colon cancer cell line LS174-T and the human umbilical vein endothelial cells (HUVECs) and compared to free gemcitabine, free isoCA-4, SQCOOH/isoCA-4 NAs, SQ-gem NAs, a mixture of gemcitabine with isoCA-4 or SQCOOH/isoCA-4 NAs, and a mixture of SQ-gem NAs with isoCA-4 or SQCOOH/isoCA-4 NAs (for experimental details, see SI). SQCOOH NAs were used as negative control. The cells were exposed to tested compounds for 3, 6, 24, and 72 h, washed with PBS, and

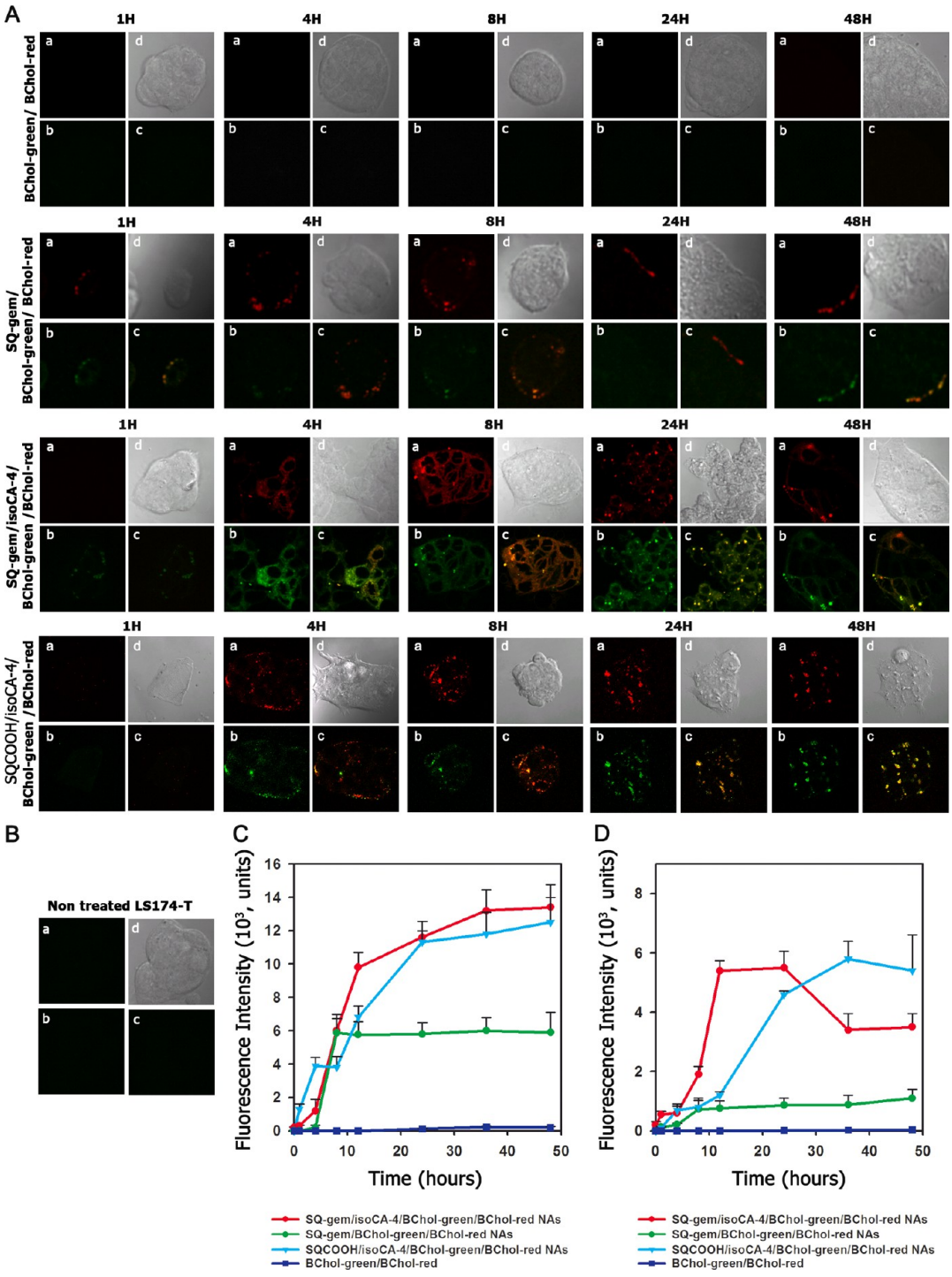

Figure 3. Cell internalization of the squalene-based nanocomposites (A,C,D). (A) Intracellular localization of SQ-gem/BChol-green/BChol-red NAs, SQ-gem/isoCA-4/BChol-green/BChol-red NAs, and SQCOOH/isoCA-4/BChol-green/BChol-red NAs in the LS174-T cells as imaged by confocal microscopy (a, BChol-red; b, BChol-green; c, merge; d, contrast phase). The mixture of free cholesterol BODIPY dyes (BChol-green with BChol-red) was used as negative control. The original magnification was ×63. (B) Nontreated cells. (C,D) Time course of nanocomposites accumulation into LS174-T cells exposed to 10 μM of fluorescently labeled SQ-gem NAs, SQCOOH/isoCA-4 NAs or SQ-gem/isoCA-4 NAs as measured by flow cytometry. The mixture of free cholesterol BODIPY dyes (BChol-green with BChol-red) was used as negative control. After incubation at different time intervals (*i.e.*, 1, 4, 8, 12, 24, 36, and 48 h), the cells were trypsined and then analyzed on a FACScan flow cytometer using BD Accuri CFlow Plus software (Accuri Cytometers, Ltd., UK), with argon laser as light source of 488 nm wavelength. The cells containing fluorescent nanoassemblies were selected as fluorescent positive cells on cytogram, in a total of 10 000 cells. The fluorescence of cholesterol analogues BChol-green and BChol-red was detected at 515 nm (C) and 560 nm (D), respectively. The intracellular detection of both cholesterol analogues (*i.e.*, BChol-green and BChol-red) confirms NAs uptake. Data represent the mean ± SD from triplicate independent experiments.

then analyzed by measuring the half maximal inhibitory concentration of cell proliferation. Alternatively, they were incubated in a new medium without any drug for an additional 72 h, with further test of the cell viability by MTT assay. Results showing the concentrations required to inhibit cell growth by 50% (IC_{50} values) are presented in Table S4 (SI). After 6 or 24 h drug exposure to LS174-T cells and further incubation for 72 h, the studied SQ-gem/isoCA-4 NAs showed comparable cytoxicity than that of free gemcitabine or SQ-gem NAs (Table S4 in SI). To be noted that the cytotoxic activity of isoCA-4 or SQCOOH/isoCA-4 NAs was only observed at 24 h after 72 h exposure, explained by reduced cell internalization and anticancer activity. Noteworthy, at the same incubation times (*i.e.*, 6 and 24 h) but in the absence of further 72 h incubation (with the drug-free medium), none of the NAs displayed cytotoxic activity, which may be explained by the prodrug nature of the squalenoyl gemcitabine, which requires intracellular hydrolysis before exhibiting any cytotoxic activity. After just 72 h drug exposure (without any further incubation with the drug-free medium), SQ-gem/isoCA-4 NAs displayed cytotoxicity similar to all free drug treatments, whereas other squalene-based nanoassemblies (or their mixture with free drugs) were less cytotoxic (Table S4 in SI). Similar observations were done on HUVECs, except that the contribution of isoCA-4 was more pronounced for all formulations containing this antivascular compound (Table S5 in SI). Briefly, after 3, 6, or 24 h drug exposure to HUVECs and further incubation (or not) for 72 h, the studied SQ-gem/isoCA-4 NAs showed comparable cytoxicity to all the other treatments (Table S5 in SI). The same tendency was observed also after 72 h drug exposure. It is to be noted that the IC_{50} values in HUVECs were found to be lower than those in LS174-T cells, which was consistent with previous report.[31]

Finally, the gemcitabine-induced apoptosis in LS174-T cells (for experimental details, see SI) was investigated after treatment with SQ-gem and SQ-gem/isoCA-4 NAs at IC_{50} (*i.e.*, 32 and 6 nM, respectively) and compared with free gemcitabine (4 nM) and its mixture with isoCA-4 (6 nM) (Figure S4 in SI). After 72 h treatment, Annexin V and propidium iodide (PI) staining showed comparable induction of apoptosis for NAs and free drug treated cells.

***In Vivo* Anticancer Efficacy.** The antitumor efficacy of the SQ-gem/isoCA-4 NAs has been further investigated on the human colon carcinoma xenograft model LS174-T at equimolar doses and compared to free gemcitabine, free isoCA-4, SQ-gem NAs, SQCOOH/isoCA-4 NAs, free gemcitabine mixed with free isoCA-4 or with SQCOOH/isoCA-4 NAs and SQ-gem NAs mixed with free isoCA-4 or with SQCOOH/isoCA-4 NAs. After tumors had grown to 80−100 mm^3, the animals were subjected to the different treatments using injection protocols, as explained in the Materials and Methods. As indicated in Figure 4A, the growth of LS174-T tumors was neither affected by the treatment with the control nanoassemblies made of SQCOOH (1,1′,2-tris-norsqualenic acid) nor by free isoCA-4, when compared with saline-treated tumors. Though the existing treatments have shown to significantly reduce the tumor volume, the SQ-gem/isoCA-4 NAs were by far the more efficient (93% tumor inhibition [$P < 0.001$]; day 22) (Figure 4A).

The treatment with free gemcitabine or its combination with free isoCA-4 reduced the volume of LS174-T tumor by only 32% ($p < 0.001$) and 60% ($p < 0.001$), respectively. On the contrary, the combination of free isoCA-4 with SQ-gem NAs did not improve antitumor activity of SQ-gem NAs. Indeed, the treatment with SQ-gem NAs alone or its mixture with free isoCA-4 reduced the volume of LS174-T tumors by only 73% ($P < 0.001$) and 71% ($P < 0.001$), respectively. Surprisingly, if the encapsulation of free isoCA-4 into squalenic acid nanoassemblies improved the antitumor activity of this compound (*i.e.*, 47% tumor inhibition *versus* 8% for the free drug), its mixture with gemcitabine (either free or as SQ-gem nanoassemblies) displayed only moderate antitumor activity enhancement (55% tumor inhibition for SQCOOH/isoCA-4 NAs+gemcitabine and 75% tumor inhibition for SQCOOH/isoCA-4 NAs+SQ-gem NAs) and never reached tumor inhibition reached by SQ-gem/isoCA-4 NAs (93%). Relative body weight loss was also monitored throughout the different treatments (Figure 4B). Absolute weight loss was observed in the control and free drug-treated mice (*i.e.*, gemcitabine, isoCA-4 and gemcitabine+isoCA-4) but not after SQ-gem or SQ-gem/isoCA-4 NA treatment. Indeed, the mice treated with gemcitabine or its combination with isoCA-4 and SQCOOH/isoCA-4 NAs exhibited significant weight loss (12−15%), below the usual value of the maximal tolerable dose (MTD) (*i.e.*, 10%), showing the toxicity of these treatments. IsoCA-4 or SQCOOH/isoCA-4 NAs treated mice demonstrated comparable absolute weight loss than control non-treated mice (∼ 6%), which was associated with tumor aggressiveness. On the contrary, the mice treated with the SQ-gem/isoCA-4 NAs nanocomposites slightly increased their body weight (∼ +3%), which supports both the efficient anticancer activity of these nanoassemblies (since the absence of weight loss reflects the reduced tumor aggressiveness) and the absence of adverse effects. On the contrary, the mixture of SQ-gem NAs with free isoCA-4 or with SQCOOH/isoCA-4 NAs exhibited slight weight loss (9 and 2%, respectively). In a nutshell, the multitherapy SQ-gem/isoCA-4 nanoassemblies displayed the more efficient anticancer pharmacological activity with almost complete suppression of tumor growth and absence of toxicity related to weight loss. Toxicity of SQ-gem/isoCA-4 NAs has been further investigated by histopathology of major organs (*i.e.*, liver, kidneys, spleen, small intestine,

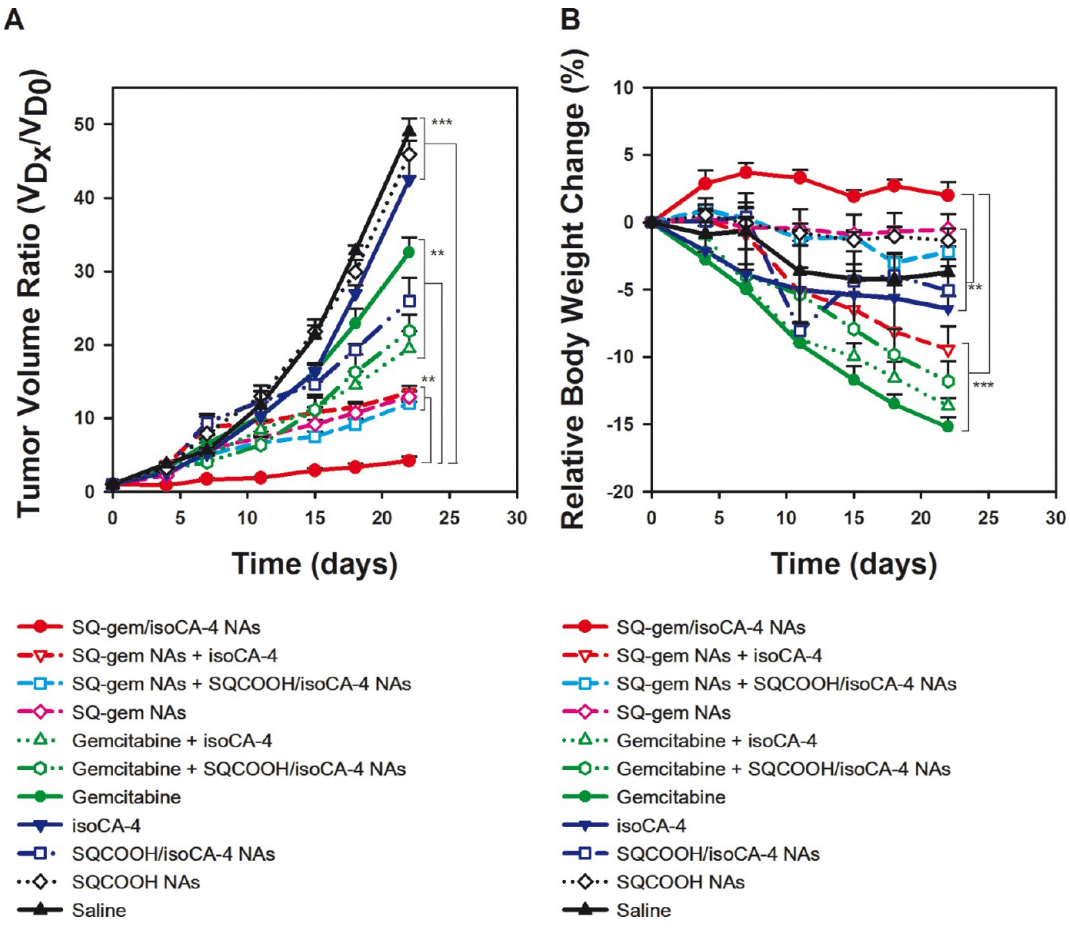

Figure 4. Tumor growth inhibition after multidrug treatment of mice bearing human colon (LS174-T) tumor. All groups received four intravenous injections on days 0, 4, 8, and 12 in the lateral tail vein of either (i) SQ-gem/isoCA-4 NAs, (ii) SQ-gem NAs, (iii) free gemcitabine, (iv) free isoCA-4 (30% ethanol solution), (v) free isoCA-4+free gemcitabine (30% ethanol solution), (vi) SQCOOH NAs, (vii) SQ-gem NAs+isoCA-4 (30% ethanol solution), (viii) SQCOOH/isoCA-4 NAs, (ix) SQCOOH/isoCA-4 NAs+SQ-gem NAs, (x) SQCOOH/isoCA-4 NAs+free gemcitabine, or (xi) saline 0.9%. All treatments were performed at the same dose, *i.e.*, at 20 μmol/kg, except the control saline 0.9%. Tumor volume (A) and body weight (B) were regularly measured during the experimental period. The values are the mean ± SD (n = 10). After 22 days, statistical analysis of tumor volumes showed superior antitumor efficacy of SQ-gem/isoCA-4 nanocomposites compared to all other treatments (n = 10, $^{**}P < 0.01$, $^{***}P < 0.001$).

brain, heart, and lungs), but no significant toxicity was observed at the used dose schedule (Table S6, Figures S7−S14 in SI).

Tumor Distribution and Pharmacokinetic Studies. In order to explain the better anticancer activity and lower toxicity of squalene-based nanocomposites *versus* free drugs, we performed pharmacokinetic and biodistribution studies in LS174-T tumor-bearing nude mice (Table S7 and Table S8 in SI). Bioavailability, calculated from the area under the plasma concentration *versus* time curve from 0 to ∞ hours ($AUC_{0-\infty}$), was compared for SQ-gem/isoCA-4 NAs *versus* the free drug mixture (gemcitabine+isoCA-4). After administration of SQ-gem/isoCA-4 nanocomposites, the $AUC_{0-\infty}$ of the global gemcitabine pool in plasma (*i.e.*, gem+SQ-gem) was 6.8-times higher than that resulting from the injection of gemcitabine+isoCA-4 (mean = 490.1 *versus* 72.5 nmol mL^{-1} h^{-1}, difference = 417.6 nmol mL^{-1} h^{-1}) (Figure 5A; Table S7 in SI). On the contrary, $AUC_{0-\infty}$ of isoCA-4 was 2.7-times lower (mean = 102.1 *versus* 272.5 nmol mL^{-1} h^{-1}, difference = −170.4 nmol mL^{-1} h^{-1}) (Figure 5A; Table S7 in SI). Concerning tissue distribution (Figures 5B and 5C; Table S8 in SI), the $AUC_{0-\infty}$ of the whole gemcitabine pool in tumor (*i.e.*, gem+SQ-gem) after injection of SQ-gem/isoCA-4 NAs was 7.9-times higher than that resulting from the injection of gemcitabine+isoCA-4 as free drugs (mean = 1059.9 *versus* 134.5 nmol g^{-1} h^{-1}, difference = 925.4 nmol g^{-1} h^{-1}) (Figure 5C; Table S8 in SI). However, $AUC_{0-\infty}$ of isoCA-4 in tumor was 20.6-times lower with NAs than after injection of gemcitabine+isoCA-4 as free drugs (mean = 30.8 *versus* 634.0 nmol g^{-1} h^{-1}, difference = −603.2 nmol g^{-1} h^{-1}) (Figure 5B; Table S8 in SI).

These results may be summarized as follows: (i) the administration of the SQ-gem/isoCA-4 nanoassemblies induced much higher plasma concentrations and prolonged circulation time of the gemcitabine pool (*i.e.*, gem+SQ-gem) than after the administration of the two drugs free; (ii) plasma concentrations of isoCA-4

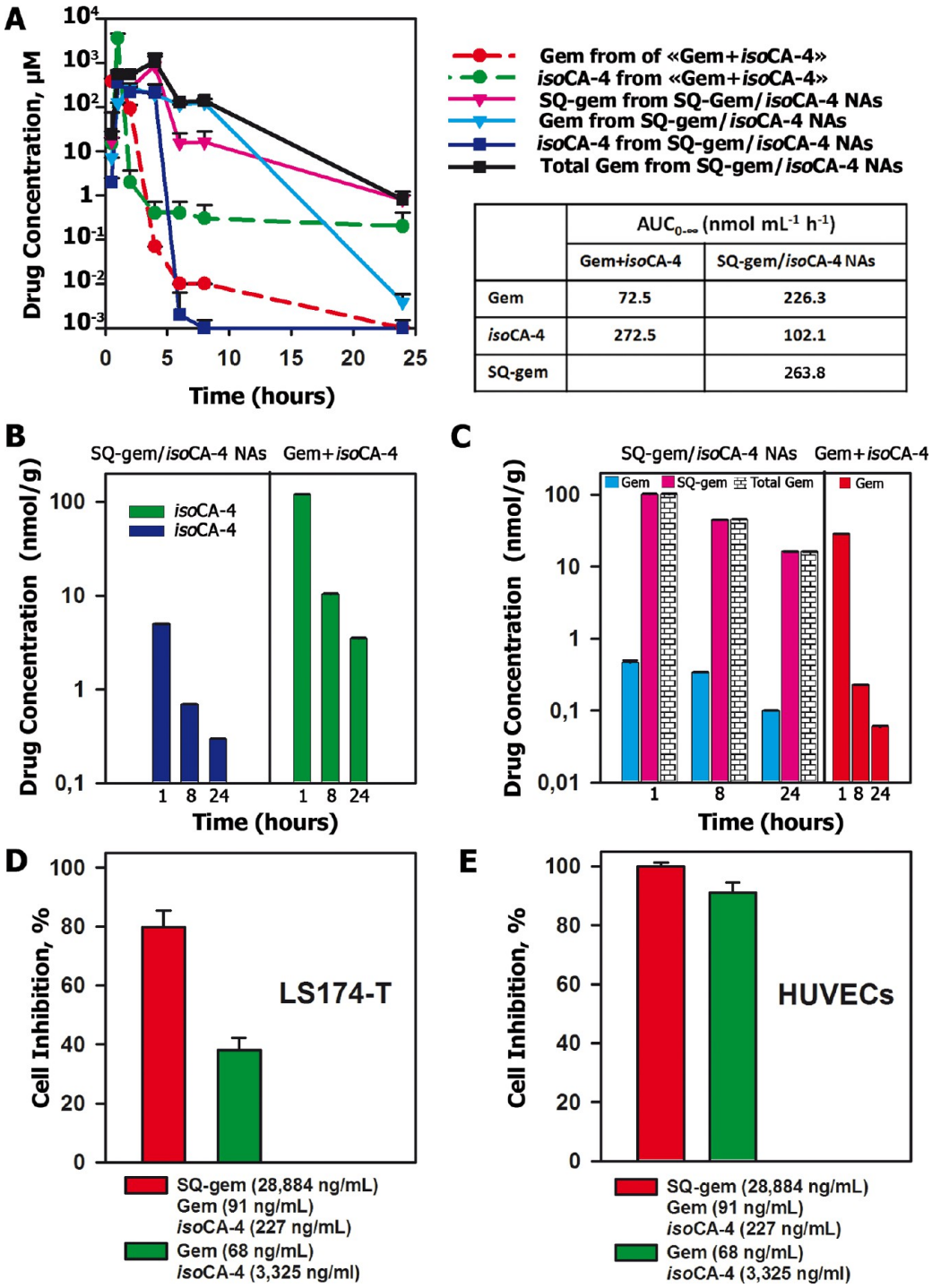

	$AUC_{0-\infty}$ (nmol mL^{-1} h^{-1})	
	Gem+*iso*CA-4	SQ-gem/*iso*CA-4 NAs
Gem	72.5	226.3
*iso*CA-4	272.5	102.1
SQ-gem		263.8

Figure 5. Pharmacokinetic and tumor distribution (A–C) and antitumor activity *in vitro* (D,E) of SQ-gem/isoCA-4 NAs or free drugs mixture (*i.e.*, gem+isoCA-4). (A) Plasma concentrations of gemcitabine, SQ-gem and isoCA-4 after a single injection of SQ-gem/isoCA-4 NAs (50 μmol/kg, continued lines) or free drugs mixture (gemcitabine and isoCA-4, 50 μmol/kg, dotted lines), as a function of time postinjection. The values are the mean ± SD (n = 5). (B) Tumor concentrations of isoCA-4 at 1, 8, and 24 h after a single injection of either SQ-gem/isoCA-4 NAs (50 μmol/kg) or the free drugs mixture (gemcitabine and isoCA-4, 50 μmol/kg). (C) Tumor concentrations of gemcitabine and SQ-gem at 1, 8, and 24 h after a single injection of SQ-gem/isoCA-4 NAs (50 μmol/kg) or free drugs mixture (gemcitabine and isoCA-4, 50 μmol/kg). The values are the mean ± SD (n = 5). (D,E) Cell inhibition of the LS174-T cell line (D) or HUVECs (E) exposed to exactly the same concentrations of drugs than those found *in vivo* in the tumor nodules after treatment with either SQ-gem/isoCA-4 NAs or free drugs mixture, at 8 h post administration (*i.e.*, 91 ng/mL [0.35 μM] gem + 28 884 ng/mL [44.7 μM] SQ-gem + 227 ng/mL [0.72 μM] isoCA-4 *versus* 68 ng/mL [0.23 μM] gem + 3325 ng/mL [10.5 μM] isoCA-4). After exposure to the drugs for 6 h, the cells were washed by PBS and incubated in a new medium without any drug up to 72 h with further analysis by MTT assay.

raised higher values after administration of the drugs free than after treatment with SQ-gem/isoCA-4 nanoassemblies; and (iii) the pool of gemcitabine in the tumors was dramatically increased, but the concentration of isoCA-4 decreased after treatment with SQ-gem/isoCA-4 nanoassemblies, comparatively to the administered mixture of gemcitabine with isoCA-4.

To explain the improved antitumor activity of SQ-gem/isoCA-4 NAs in spite of the lower accumulation of isoCA-4 in tumors, a cytotoxicity study has been performed by exposing the human colon cancer cells (LS174-T) and the HUVECs to exactly the same concentrations of drugs as those found in the tumor nodules *in vivo*, at 8 h post administration (*i.e.*, 91 ng/mL [0.35 μM] gem + 28 884 ng/mL [44.7 μM] SQ-gem + 227 ng/mL [0.72 μM] isoCA-4 *versus* 68 ng/mL [0.23 μM] gem + 3325 ng/mL [10.5 μM] isoCA-4, corresponding to the administration of NAs and free drugs, respectively). As shown in Figure 5D,E, these higher gemcitabine and SQ-gem concentrations and lower isoCA-4 concentrations obtained after SQ-gem/isoCA-4 NAs treatment induced the efficient killing of both cancer cells and endothelial cells (80 and 100%, respectively), whereas lower gemcitabine concentrations, even with higher dosage of isoCA-4, as those obtained after treatment with the free drugs, failed to efficiently kill cancer cells (only 38%). Indeed, endothelial cells were very sensitive to isoCA-4 which was not the case of LS174-T human colon cancer cells toward gemcitabine. In other words, very low doses of isoCA-4 were sufficient to induce 100% mortality of endothelial cells, whereas higher concentrations of gemcitabine were needed to efficiently kill cancer cells.

Morphological and Immunohistochemical Analysis of Tumor Biopsies. The antitumor efficacy of squalenoyl-based nanocomposites was confirmed also by morphological and immunohistochemical analysis of tumor biopsies. Immunohistochemical analysis of biopsies demonstrated enlarged cells with necrotic changes only in squalene-based nanoassemblies-treated tumor tissues (Figure 6A). The TUNEL staining of tumor biopsies sections (5 μm), which is a common method for detecting the DNA fragmentation that results from apoptotic signaling cascades, was used to assess the induction of apoptosis by the different treatments *in vivo* (Figure 6B). The mean proportion of TUNEL positive cells/field (red color, Figure 6B) for SQ-gem/isoCA-4 NAs, gemcitabine+isoCA-4, gemcitabine+SQCOOH/isoCA-4 NAs, SQ-gem NAs+isoCA-4, SQ-gem NAs+SQCOOH/isoCA-4 NAs, SQ-gem NAs, SQCOOH/isoCA-4 NAs, free gemcitabine and free isoCA-4 treated groups were 21.4, 0.6, 0.6, 11.8, 12, 9.5, 0.4, 0.6, and 0.4%, whereas tumors from saline or SQCOOH NAs control groups had a mean proportion of 0.4% of TUNEL positive cells/field (Figure 6H). Among the different signaling pathways of programmed cell death, caspase-3 plays a central role in the execution-phase of cell apoptosis. Immunostaining of the active form of caspase-3 protease revealed major caspase-3 activation (42.8%) in SQ-gem/isoCA-4 NAs mice only (Figure 6C,G). Tumors from mice receiving the SQ-gem NAs+isoCA-4, SQ-gem NAs+SQCOOH/isoCA-4 NAs, gemcitabine+SQCOOH/isoCA-4 NAs, SQCOOH/isoCA-4 NAs, SQ-gem NAs, free gemcitabine, free isoCA-4, or the mixture of the gemcitabine with isoCA-4 had a mean value of only 19, 23.8, 3.8, 2.4, 21.4, 0.6, 0.8, and 1.2% positive cells/field respectively, whereas tumors from saline or SQCOOH NAs control groups had a mean value of 0.5% of caspase-3 positive cells/field. The high activation of apoptosis and caspase-3 protease by SQ-gem/isoCA-4 NAs in the tumor may be explained by the delivery inside the cells of the two active compounds from nanocomposites, which led to a synergistic antitumor effect of the antiproliferative agents isoCA-4 and gemcitabine. This hypothesis was confirmed by the staining of proliferating cells by Ki-67 antibody for each biopsy specimen (Figure 6D,F).

The Ki-67 protein (also known as MKI67) is a cellular marker for cell proliferation.[32] During interphase, the Ki-67 antigen can only be detected within the cell nucleus, whereas in mitosis, most of the protein relocates onto the surface of the cell membrane. As shown in Figure 6F, tumors from mice receiving SQ-gem/isoCA-4 NAs, SQ-gem NAs, SQ-gem NAs+isoCA-4, SQ-gem NAs+SQCOOH/isoCA-4 NAs, gemcitabine+SQCOOH/isoCA-4 NAs, SQCOOH/isoCA-4 NAs, free gemcitabine, free isoCA-4, or the mixture of gemcitabine with isoCA-4 had mean values of respectively 14.3, 33.3, 31.9, 38, 69, 77, 81, 83, and 74% Ki-67 positive cells/field, whereas tumors receiving saline or SQCOOH NAs had mean values of 92 and 88% Ki-67 positive cells/field, respectively. Finally, the antineovasculature effect of the squalene-based nanocomposites was confirmed by immunostaining of CD34 (Figure 6E). The CD-34 protein is a member of a family of single-pass transmembrane sialomucin proteins that show expression in early hematopoietic and vascular-associated tissue.[33] The most pronounced suppressive effect on neovasculature was clearly achieved by the SQ-gem/isoCA-4 NAs (Figure 6E,I). Tumors from mice receiving the SQ-gem/isoCA-4 NAs had a mean value of only 2.3% vessel area/field, whereas tumors from the all other groups had a mean value of 10.5% vessel area/field. Although isoCA-4 is a new and efficient antivascular and antiproliferative bifunctional compound *in vitro*, its application *in vivo* is severely limited because of its insolubility in water medium.[27,28] Thus, as assessed by all investigated immunohistological markers, the delivery of this lipophilic compound by squalene-based nanoassemblies led to effective neovascularization disruption and tumor cell inhibition.

DISCUSSION

In previous reports,[21,34] we have taken advantage of the remarkable dynamically folded conformation of squalene to chemically conjugate this lipid with various therapeutic molecules in order to construct

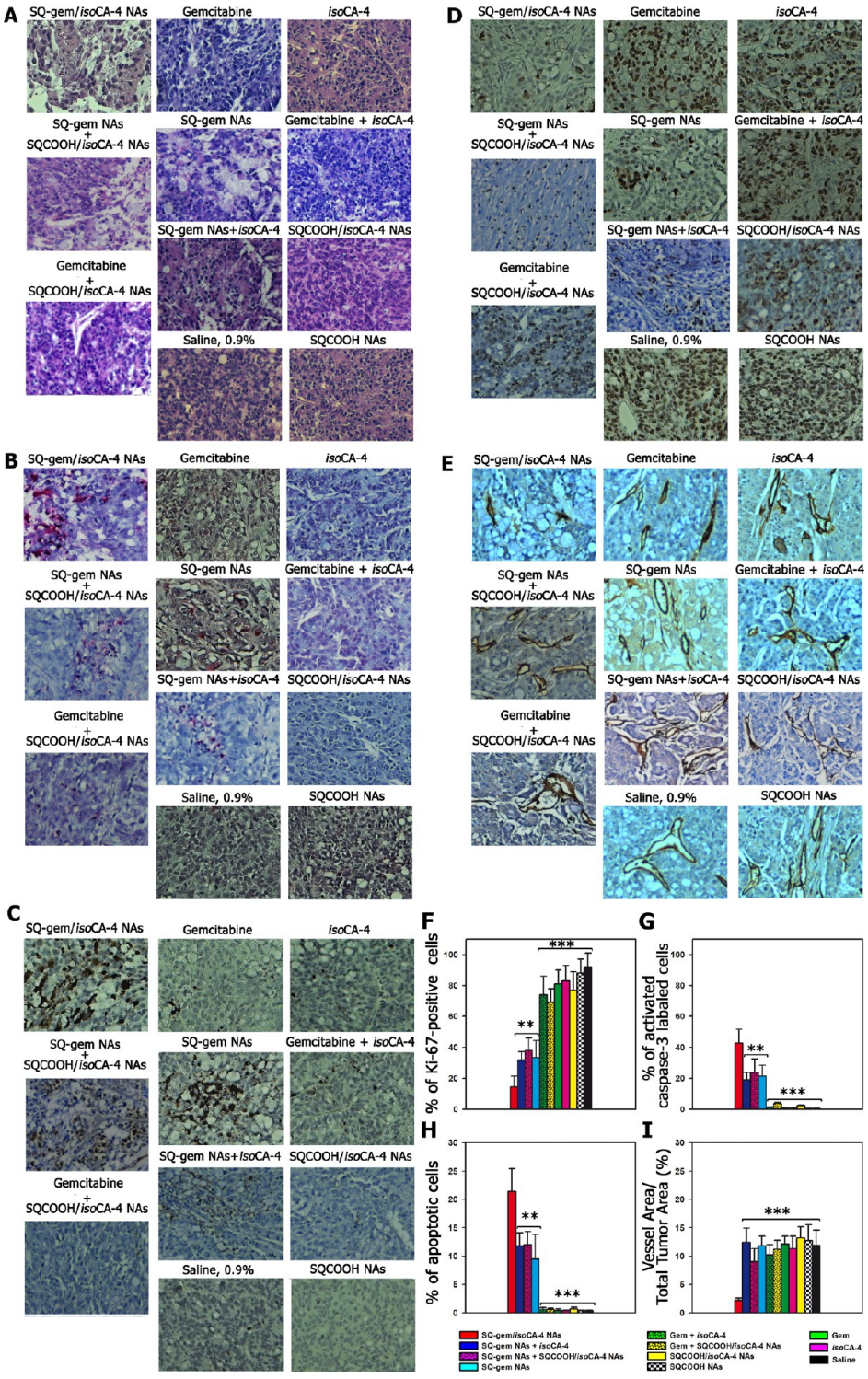

Figure 6. Immunohistochemical staining of tumor tissues derived from injected human colon (LS174-T) cancer cells. The tumors were treated on days 0, 4, 8, and 12 in the lateral tail vein by (i) SQ-gem/isoCA-4 NAs, (ii) SQ-gem NAs, (iii) free gemcitabine, (iv) free isoCA-4 (30% ethanol solution), (v) free isoCA-4+free gemcitabine (30% ethanol solution), (vi) SQCOOH NAs, (vii) SQ-gem NAs+isoCA-4 (30% ethanol solution), (viii) SQCOOH/isoCA-4 NAs, (ix) SQCOOH/isoCA-4 NAs+SQ-gem NAs, (x) SQCOOH/isoCA-4 NAs+free gemcitabine, or (xi) saline 0.9% and excised at day 14. (A) Hematoxylin/eosin/safranin staining (HES) for morphology study, (B) apoptotic cells (red), TUNEL staining, (C) caspase-3 staining, (D) proliferated cells, Ki-67 staining, and (E) CD34 staining for detection of the tumor vasculature. (F−I) Quantification: (H) TUNEL, (G) caspase-3 and (F) Ki-67-positive cells in the tumor tissue sections and (I) percentage of the vessel area with reference to the total tumor area. Five representative fields were chosen for counting. The average count within each region was used for statistical analysis. Necrotic fields were excluded. The values are the mean ± SD ($n = 5$, $^{**}P < 0.01$, $^{***}P < 0.001$).

nanoassemblies of 100−300 nm with very high drug payload. This so-called "squalenoylation" concept has been applied with success to gemcitabine, among other anticancer compounds. In the current study, we have investigated whether the squalenoyl prodrug nanoassemblies could be used for the encapsulation of an additional lipophilic antivascular compound, allowing the design of multitherapeutic nanocomposites capable of improving the therapeutic index of combined therapies. Using gemcitabine as a drug model, we designed nanoassemblies composed of both the anticancer SQ-gem bioconjugate and the antivascular agent isoCA-4 (SQ-gem/isoCA-4 NAs). The nanocomposites were prepared by an easy self-assembly process, consisting in the single addition of an ethanolic solution of SQ-gem and isoCA-4 into water. The resulting suspensions of SQ-gem/isoCA-4 contained very stable and narrowly dispersed nanoassemblies (PSD < 0.1) of 142 nm in diameter, with impressive drug loading, since the addition of gemcitabine and isoCA-4 represented 60% of the total nanoparticle weight. Noteworthy, the tentative to prepare multidrug liposomes with sufficient payload of both gemcitabine and isoCA-4 failed because of the low gemcitabine loading and the poor solubility of isoCA-4 in the organic solvents used for liposomal preparation. Importantly, it was observed that the incorporation of the lipophilic isoCA-4 into SQ-gem NAs contributed to stabilize them. It is hypothesized that the already previously described[30] inverted hexagonal phases of the SQ-gem NAs turned to an amorphous more stable structure after loading with the lipophilic compound isoCA-4. Further X-ray diffraction studies by SAXS will be performed to confirm this point.

In vitro biological assessment showed that, after 72 h drug incubation with human colon carcinoma cell line LS174-T and human umbilical vein endothelial cells (HUVECs), the squalene-based nanocomposites displayed notable cytotoxicity, quite comparable to the free drugs alone or in mixture (IC_{50} below the micromolar range, Table S4 and Table S5 in SI). Concerning the measure of the apoptotic fraction, no important differences were noted between SQ-gem/isoCA-4 NAs and the other treatments too (Figure S4 in SI), whereas these multidrug SQ-gem/isoCA-4 nanoassemblies displayed much better anticancer efficacy *in vivo* (Figure 4). This discrepancy may be explained by the different experimental conditions: *in vitro* experiments are performed on short time periods (72 h), whereas the *in vivo* experiments are running over weeks. Therefore, *in vitro* experiments are likely more sensitive to the "prodrug" effect (*i.e.*, the time needed to release the pharmacologically active gemcitabine), since only 11 and 23% of gemcitabine were released after 72 h from SQ-gem NAs and SQ-gem/isoCA-4 NAs, respectively (Figure 2C,D). This explains why, comparatively to the free drug, the squalene-based nanoassemblies were comparatively less efficient *in vitro* than *in vivo*.

As shown in Figure 3 and Figure S3 (SI), it was observed that the multitherapy SQ-gem/isoCA-4 NAs were efficiently captured by LS174-T cancer cells and HUVECs. Interestingly, thanks to a double fluorescent labeling approach, it was found that SQ-gem NAs and SQ-gem/isoCA-4 NAs interacted very differently with cells: whereas SQ-gem NAs were located only in the cell membrane and cannot accumulate intracellularly as intact nanoparticles, the SQ-gem/isoCA-4 NAs displayed a higher cell association with a clear intracellular cytoplasmic localization (Figure 3A, Figure S3A in SI). The cell membrane localization of SQ-gem was in accordance with previously published data, which have demonstrated that because of their inverted hexagonal supramolecular organization, SQ-gem nanoparticles disassembled extracellularly or at the cell membrane and were unable to be cell internalized by endocytosis.[26,35] We suggest that the incorporation of lipophilic isoCA-4 into SQ-gem NAs structurally stabilized the nanoassemblies by losing their hexagonal phase organization, thus allowing their intracellular capture as intact nanoassemblies. Despite the improved intracellular capture of SQ-gem/isoCA-4 nanocomposites by cancer cells, they exerted similar cytotoxicity than SQ-gem NAs. This may be explained in the light of the drug release experiments, which showed that the release of the pool of gemcitabine molecules was faster from SQ-gem NAs than from SQ-gem/isoCA-4 NAs, likely because of the lower stability/lipophilicity of the former nanoformulation (Figures 2C,D). The faster release of the pool of gemcitabine molecules from SQ-gem NAs could, therefore, compensate for the effect of the rapid accumulation of SQ-gem/isoCA-4 NAs in the cancer cells.

The antitumor efficacy of the squalene-based nanocomposites was then investigated *in vivo* on a human colon vascularized (LS174-T) carcinoma xenograft model in mice, and compared to the other treatments combinations (*i.e.*, gemcitabine, isoCA-4, SQ-gem NAs, gemcitabine mixed with isoCA-4 or with SQCOOH/isoCA-4 NAs and SQ-gem NAs mixed with isoCA-4 or with SQCOOH/isoCA-4 NAs). All treatments were performed at equimolar doses of drugs (20 μmol equiv of gemcitabine and/or isoCA-4). The SQgem/isoCA-4 NAs showed considerable improvement in antitumor activity (*i.e.*, 93% tumor growth inhibition), as compared to SQ-gem NAs (73%), to SQ-gem NAs+isoCA-4 (71%), to gemcitabine (32%), or to gemcitabine+isoCA-4 (60%). Treatments with isoCA-4, saline or SQCOOH NAs alone displayed no antitumor activity on human LS174-T colon cancer. Clearly, the dual-drug nanocomposite SQ-gem/isoCA-4 exhibited a better antitumor effect than single-drug NAs or their mixtures, suggesting a synergistic effect of isoCA-4 and gemcitabine. All the immunohistochemical markers have confirmed the superiority of the multitherapy nanomedicine, since SQ-gem/isoCA-4 NAs demonstrated the strongest antineovasculature and antiproliferative activities, and the

most tumor cell apoptosis by caspase-3 pathway activation (Figure 6). Noteworthy, the improved anticancer activity of SQ-gem/isoCA-4 NAs was obtained with lower toxicity than the parent drugs injected alone or mixed together (Figure 4B).

Such increased anticancer activity of squalene-based nanocomposites may be explained by the pharmacokinetic and biodistribution data. Indeed, the administration of gemcitabine and isoCA-4 as squalenoylated multidrug nanoassemblies led to a dramatic increase of the global gemcitabine pool in the tumor nodules but to a lower tumoral distribution of isoCA-4, as compared with the coadministration of gemcitabine and isoCA-4 as free drugs. When reproduced *in vitro*, the higher gemcitabine and SQ-gem concentrations and lower isoCA-4 concentrations, provided by the treatment with the nanocomposites, induced the efficient killing of both cancer cells and endothelial cells, whereas lower gemcitabine concentrations, even with higher dosage of isoCA-4, resulting from free drug treatment, failed to kill cancer cells. Endothelial cells were, indeed, very sensitive to isoCA-4 which was not the case of human LS174-T cancer cells toward gemcitabine. Thus, these results have clearly evidenced that the benefit of the multidrug nanoassemblies resulted from a dramatic modification of the pharmacokinetic and biodistribution profiles of the two biologically active compounds, in comparison to their administration just as free drugs.

Furthermore, another major advantage of the multidrug nanoassemblies approach lies on the possibility to administer intravenously the water nonsoluble compound isoCA-4. Indeed, due to its partitioning coefficient, isoCA-4 self-assembled in a very easy manner with the SQ-gem nanoparticles, allowing the safe intravenous administration of this compound. In the pharmacokinetic and pharmacodynamic experiments performed, free isoCA-4 could be administered only by using an important volume of solvent (*i.e.*, ethanol), which would not be affordable for humans.

CONCLUSIONS

In summary, this study demonstrates that efficient multitherapy nanomedicine may be designed by the single enrichment of gemcitabine-squalene nanoassemblies with a lipophilic antiangiogenic agent. There is a consensus in the pharmaceutical field that the complicated architecture and design of many proposed multifunctional nanodevices and their tricky scaling-up is a brake to their translation from research to clinic. In this context, due to its easiness, the present concept may represent a step ahead toward a multidrug nanomedicine better tailored for a realistic pharmaceutical development. This approach could be applied to other pairs of squalenoylated nanoassemblies with other non-water-soluble drugs, thus broadening the application of the "squalenoylation" concept in oncology and improving the antitumor efficacy of the insoluble anticancer drugs *in vivo*. This strategy of combination therapy deserves further investigation for personalized cancer treatment.

MATERIALS AND METHODS

Materials. Gemcitabine was purchased from Sequoia Research Product, Ltd. (UK). Squalene, 3-[4,5-dimethylthiazol-2-yl]-3,5-diphenyl tetrazolium bromide (MTT), 2′-deoxycytidine, colchicine and sodium acetate were purchased from Sigma-Aldrich Chemical Co. (St. Quentin Fallavier, France). Tetrahydrouridine was purchased from Merck Chemicals, Ltd. (Nottingham, UK). All solvents were purchased from Carlo Erba (Val-de-Reuil, France). CholEsteryl BODIPY 542/563, CholEsteryl BODIPY FL, Annexin V-FITC apoptosis assay kit and cell culture reagents were purchased from Invitrogen-Life Technologies (Cergy Pontoise, France). The synthesis of squalenoyl-gemcitabine (SQ-gem), 1,1′,2-tris-nor-squalenic acid and diarylethylene isoCA-4 has been previously reported by us (Figure 1).[21,27]

Animals. Six-eight-week old female athymic nude mice were purchased from Harlan Laboratory. All animals were housed in appropriate animal care facilities during the experimental period and were handled according to the principles of laboratory animal care and legislation in force in France. All *in vivo* studies were performed in accordance with a protocol approved by the Ethical Committee of the Institut Gustave Roussy (CEEA IRCIV/IGR No. 26, registered with the French Ministry of Research).

Cell Culture. Human colon carcinoma cell line LS174-T and human umbilical vein endothelial cells (HUVECs) were obtained from the LCS Collection (Germany) and maintained as recommended. Briefly, LS174-T cells were maintained in MEM medium. HUVEC cells were grown in Dulbecco's minimal essential medium (DMEM)−Glutamine medium. All media were supplemented with 10% (v/v) heat-inactivated fetal calf serum (FCS) (56 °C, 30 min), penicillin (100 U/mL) and streptomycin (100 U/mL). Cells were maintained in a humid atmosphere at 37 °C with 5% CO_2.

The cell line LS174-T was established from a Duke's type B adenocarcinoma of the colon. The tissue was minced and cultured without transfer for 10 months. The cells have microvilli and intracytoplasmic vacuoles. LS174-T cells have been shown also to secrete large amounts of matrix metalloproteinases (MMPs) and to be highly tumorigenic.[36] Tumors developed within 21 days at 100% frequency (5/5) in nude mice inoculated subcutaneously with 10^7 cells.

Preparation and Characterization of the SQ-gem/isoCA-4 Nanoassemblies. Squalenoyl nanocomposites were prepared using the nanoprecipitation method after optimization as indicated in Supporting Information and the best formulation was used for further *in vitro* and *in vivo* studies. Briefly, a solution of SQ-gem in ethanol (200 μL at 25 μmol mL^{-1}) alone or mixed with a solution of isoCA-4 (200 μL at 25 μmol mL^{-1}) was added dropwise under stirring (1000 rpm) into 1 mL of distilled water. Nanoprecipitation of the SQ-gem or SQ-gem/isoCA-4 nanoassemblies occurred spontaneously. Ethanol was completely evaporated under a vacuum using a Rotavapor at 20 °C to obtain an aqueous suspension of SQ-gem NAs or SQ-gem/isoCA-4 NAs (5 μmol mL^{-1}). Squalenic acid nanoassemblies (SQCOOH NAs) (5 μmol mL^{-1}) and Squalenic acid nanoparticles loaded with isoCA-4 (SQCOOH/isoCA-4 NAs) at a SQCOOH: isoCA-4 molar ratio of 2:1 (5 μmol mL^{-1} isoCA-4), used as controls, were prepared employing exactly the same procedure as described above for SQ-gem and SQ-gem/isoCA-4 NAs. The nanoassemblies made of SQCOOH/isoCA-4, SQ-gem or SQ-gem/isoCA-4 were fluorescently labeled and prepared in a similar manner. Practically, SQCOOH/isoCA-4 (25 μmol in isoCA-4), SQ-gem (25 μmol) or SQ-gem/isoCA-4 (25 μmol) were mixed with 250 nmol of CholEsteryl BODIPY 542/563 (BChol-red) and

CholEsteryl BODIPY FL (BChol-green) in ethanol and added dropwise under stirring (1000 rpm) into 1 mL of distilled water. Ethanol was then completely evaporated as described above.

The size of the nanoassemblies was determined at 20 °C by quasielastic light scattering (QELS) with a nanosizer (Zêtasizer Nano ZS Malvern; Malvern Instruments SA, Orsay, France) after 1:10 dilution in water. All the squalenoyl gemcitabine nanoassemblies prepared in conditions as described above gave stable suspensions with size in the range 100−150 nm (PSD < 0.1) (Table 1).

The morphology of the different nanoassemblies was examined by cryogenic temperature transmission electron microscopy (cryo-TEM). Briefly, one drop (5 μL) of the squalenoyl gemcitabine nanoassemblies suspension (5 μmol mL^{-1}) was deposited onto a perforated carbon film mounted on a 200-mesh electron microscopy grid. Most of the drop was removed with a blotting filter paper, and the residual thin films remaining within the holes were vitrified after immersion in liquid ethane. The specimen was then transferred using liquid nitrogen to a cryospecimen holder and observed using a JEOL FEG-2010 electron microscope.

To study the colloidal stability of the various NAs suspensions, the samples were maintained at 4 °C; size and PSD were measured at different time points during 90 days.

The release of gemcitabine and isoCA-4 from squalenoyl gemcitabine nanoassemblies was investigated after incubation in heat inactivated fetal calf serum. At different time intervals (*i.e.*, 0.5, 1, 4, 8, 24, 48, and 72 h), aliquots (300 μL) of the incubation medium were removed and ultracentrifuged (15000*g*, 30 min). IsoCA-4, gemcitabine and SQ-gem were quantified by UPLC−MS/MS, as described in Supporting Information.

Cell Internalization of SQ-gem, SQCOOH/isoCA-4, and SQ-gem/isoCA-4 NAs. HUVECs or LS174-T cells were cultured on a coverslip in a culture dish for 24 h to achieve approximately 40% confluence. Cells were then treated for different time periods with 10 μM concentration of either SQ-gem NAs, SQCOOH/isoCA-4 NAs or SQ-gem/isoCA-4 NAs, all fluorescently labeled with equimolar mixture of BChol-red and BChol-green, as described above. After treatment, the cells were washed with Dulbecco's PBS, incubated with 3% paraformaldehyde in PBS for 20 min at room temperature, and then washed four times with PBS.[37] Coverslips were mounted on glass slides with *p*-phenylenediamine in glycerol.[37] Cells were imaged with a confocal fluorescence microscope (Leica TCS SP2, Leica, Wetzlar, Germany) equipped with a 63×/1.3 NA oil immersion lens. The following wavelengths were used: excitation at 488 nm and detection through a 515 nm filter for BChol-green, and excitation at 543 nm and detection through a 560 nm filter for BChol-red.

To monitor real-time cell uptake kinetics of either SQ-gem/BChol-green/BChol-red NAs, SQ-gem/isoCA-4/BChol-green/BChol-red NAs or SQCOOH/isoCA-4/BChol-green/BChol-red NAs, HUVECs or LS174-T cells were cultured on 6-well plates for 24 h to achieve 60−80% confluence. The fluorescently labeled nanoassemblies were then added at a final concentration of 10 μM to each well. After incubation at different time intervals, the cells were trypsined and then analyzed on a FACScan flow cytometer using BD Accuri CFlow Plus software (Accuri Cytometers, Ltd., UK), with argon laser as light source of 488 nm wavelength. The cells containing fluorescent nanoassemblies were selected as fluorescent positive cells on cytogram, in a total of 10 000 cells. For detection of BChol-green or BChol-red fluorescence, the emission spectrum was measured at 515 or 560 nm, respectively.

***In Vivo* Study Design.** The antitumor efficacy of composite SQ-gem/isoCA-4 NAs was evaluated comparatively to free drugs or to other squalenoylated nanoassemblies (alone or combined), at drug's equimolar doses on LS174-T-bearing mice. Practically, 200 μL of the LS174-T cell suspension, equivalent to 1 × 10^6 cells, were injected subcutaneously into nude mice toward the upper portion of the right flank, to develop a solid tumor model. Tumors were allowed to grow until reaching a volume ∼90 mm^3 before initiating the treatment. Tumor length and width were measured with calipers, and the tumor volume was calculated using the following equation: Tumor volume (V) = [length × width]^2/2. Tumor-bearing nude mice were randomly divided into 11 groups of 10 each, and all groups received four intravenous injections on days 0, 4, 8, and 12 in the lateral tail vein of either (i) SQ-gem/isoCA-4 NAs, (ii) SQ-gem NAs, (iii) free gemcitabine, (iv) free isoCA-4 (30% ethanol solution), (v) free isoCA-4+free gemcitabine (30% ethanol solution), (vi) SQCOOH NAs, (vii) SQ-gem NAs+free isoCA-4 (30% ethanol solution), (viii) SQCOOH/isoCA-4 NAs, (ix) SQCOOH/isoCA-4 NAs+SQ-gem NAs, (x) SQCOOH/isoCA-4 NAs+free gemcitabine, or (xi) saline 0.9%. All treatments were performed at the same dose, *i.e.*, at 20 μmol/kg, except the control saline 0.9%. The injected volume was 10 μL/g of body weight. The mice were monitored regularly for changes in tumor size and weight.

Immunohistochemical Analysis of Xenografts. Tumors were excised at day 14, fixed in Finefix (Milestone, Italy), paraffin-embedded, and cut into 5-μm-thick sections. Hematoxylin/eosin/safranin (HES) staining was performed on all of the xenografts for analysis of morphology. For the evaluation of the intratumoral vascular density, anti-CD-34 (1:200; Abcam, Cambridge, United Kingdom) immunohistochemistry, detecting human endothelial cells was performed for all tumors on a large section that included the total tumor. For cell proliferation analysis, sections were incubated with Ki-67 antibody (1:200; Abcam). Cellular apoptosis was detected through terminal transferase dUTP nick end labeling (TUNEL) using Texas red-labeled nucleotide as per the manufacturer's instructions (Roche, Mannheim, Germany) and by caspase-3 staining (1:200; Abcam). In brief, the tumor biopsies were incubated with primary antibodies (1:200 dilution in blocking buffer (5% BSA)) for 1 h at room temperature. After washing (PBS), the sections were incubated with biotinylated secondary antibody (Jackson ImmunoResearch Laboratory, West Grove, PA) at room temperature for 30 min. Avidin−biotin complex and diaminobenzidine (DAB) reagent kits (Vector Laboratories, Burlingame, CA) were used according to the manufacturer's protocol to detect the secondary antibody. TUNEL, caspase-3 or Ki-67 positive cells or nuclei were counted per view under a light microscope (Leica Microsystems GmbH, Wetzlar, Germany) at 10-times magnification. The surface of the vessel area labeled by CD34 was quantified by ImageJ in reference to the total tumor area. Five representative fields were chosen for counting. The average count within each region was used for statistical analysis. Necrotic fields were excluded.

Histopathology. The major organs (*i.e.*, liver, kidneys, spleen, small intestine, brain, heart and lungs) of nude mice grafted with LS174-T human colon xenografts and injected with squalenoyl nanocomposites or free drugs were excised at day 22, fixed in Finefix (Milestone, Italy), paraffin-embedded, and cut into 5-μm-thick sections. Hematoxylin/eosin/safranin (HES) staining was performed on all of the organs for analysis of the specific toxicities of tested compounds (*i.e.*, (i) SQ-gem/isoCA-4 NAs, (ii) SQ-gem NAs, (iii) free gemcitabine, (iv) free isoCA-4, (v) free isoCA-4+free gemcitabine, (vi) SQCOOH NAs, (vii) SQ-gem NAs+free isoCA-4, (viii) SQCOOH/isoCA-4 NAs, (ix) SQCOOH/isoCA-4 NAs + SQ-gem NAs, (x) SQCOOH/isoCA-4 NAs+free gemcitabine, and (xi) saline 0.9%).

***In Vivo* Pharmacokinetics of SQ-gem/isoCA-4 NAs and Mixture of Free Gemcitabine with isoCA-4.** A total of 70 additional healthy nude mice were randomly assigned into two groups (n = 35 mice per group). To measure the pharmacokinetics, SQ-gem/isoCA-4 NAs (50 μmol/kg) or free drug mixture (*i.e.*, gemcitabine+isoCA-4; 50 μmol/kg) were intravenously injected into the female nude mice *via* the tail vein. Blood samples (500 μL) were collected from the tail vein into Vacutainer K3-EDTA tubes (Vacuette; Greiner-Bio One) at 30 min, 1, 2, 4, 6, 8, and 24 h after drug administration (n = 5 at each time point) and then centrifuged (2000*g* for 10 min at 4 °C) to separate the plasma which was then stored at −70 °C until gemcitabine, SQ-gem or isoCA-4 measurements (for drug quantification, see SI).

Tumor Biodistribution of SQ-gem/isoCA-4 NAs and Mixture of Free Gemcitabine with isoCA-4. For the biodistribution study, a total of 30 additional nude mice bearing LS174-T tumors (diameter ∼1 cm) were randomly assigned into two groups (n = 15 mice per group), injected intravenously with either SQ-gem/isoCA-4 NAs (50 μmol/kg) or free drug mixture (*i.e.*, gemcitabine+isoCA-4; 50 μmol/kg). In each treatment group, mice were killed by cervical dislocation at 1, 8, or 24 h after drug administration

(n = 5 at each time point). The tumor samples were collected and stored at −70 °C until gemcitabine, SQ-gem or isoCA-4 measurements (for drug quantification, see SI).

Statistical Analysis. All the data are the result of a minimum of three independent experiments. Statistics were calculated with Prism GraphPad software. The significance was calculated using a one-way Anova method, followed by Dunnett's test or with independent Student's *t* test.

Conflict of Interest: The authors declare no competing financial interest.

Acknowledgment. The research leading to these results has received funding from the European Research Council under the European Community's Seventh Framework Programme FP7/2007-2013 Grant Agreement No. 249835. UMR 8612 Couvreur's team is a member of the laboratory of excellence NANO-SACLAY, and BioCIS UMR 8076 is a member of the Laboratory of Excellence LERMIT supported by a grant from ANR (ANR-10-LABX-33). We thank the service of the animal experimentation from the IFR141 IPSIT (Châtenay-Malabry), V. Nicolas (Service Imagerie-Microscopie Confocale, IFR-141, Châtenay-Malabry, France) for expert assistance with confocal microscopy, and G. Frébourg (service of electron microscopy from IFR of Integrative Biology, Paris) for the cryo-TEM analysis. We are grateful also to Miss O. Bawa and Dr. P. Opolon (Institut Gustave Roussy, Villejuif) for analysis of organs from stained histological slides.

Supporting Information Available: Details of synthesis of 4-(*N*)-trisnorsqualenoyl-gemcitabine (SQ-gem) and isoCA-4; quantification of gemcitabine, SQ-gem and isoCA-4 in biological samples; cholesterol BODIPY dyes and drug release; cell proliferation and apoptosis assays; preparation and stability studies of squalenoyl nanocomposites; data of the cytotoxicity of squalene-based nanocomposites. This material is available free of charge *via* the Internet at http://pubs.acs.org.

REFERENCES AND NOTES

1. Ma, Y.; Shurin, G. V.; Gutkin, D. W.; Shurin, M. R. Semin. Tumor Associated Regulatory Dendritic Cells. *Semin. Cancer Biol.* **2012**, *22*, 298–306.
2. Hielscher, A. C.; Gerecht, S. Engineering Approaches for Investigating Tumor Angiogenesis: Exploiting the Role of the Extracellular Matrix. *Cancer Res.* **2012**, *72*, 6089–6096.
3. Chekhonin, V. P.; She in, S. A.; Korchagina, A. A.; Gurina, O. I. VEGF in Tumor Progression and Targeted Therapy. *Curr. Cancer Drug Targets* **2012**, *13*, 1–21.
4. Hillen, F.; Griffioen, A. W. Tumour Vascularization: Sprouting Angiogenesis and Beyond. *Cancer Metastasis Rev.* **2007**, *26*, 489–502.
5. Holash, J.; Maisonpierre, P. C.; Compton, D.; Boland, P.; Alexander, C. R.; Zagzag, D.; Yancopoulos, G. D.; Wiegand, S. J. Vessel Cooption, Regression, and Growth in Tumors Mediated by Angiopoietins and VEGF. *Science* **1999**, *284*, 1994–1998.
6. Johannessen, T. C.; Wagner, M.; Straume, O.; Bjerkvig, R.; Eikesdal, H. P. Tumor Vasculature: the Achilles' Heel of Cancer? *Expert Opin. Ther. Targets* **2013**, *17*, 7–20.
7. Rosenzweig, S. A. Acquired Resistance to Drugs Targeting Receptor Tyrosine Kinases. *Biochem. Pharmacol.* **2012**, *83*, 1041–1048.
8. Gerber, H. P.; Ferrara, N. Pharmacology and Pharmacodynamics of Bevacizumab as Monotherapy or in Combination with Cytotoxic Therapy in Preclinical Studies. *Cancer Res.* **2005**, *65*, 671–680.
9. Escorcia, F. E.; Henke, E.; McDevitt, M. R.; Villa, C. H.; Smith-Jones, P.; Blasberg, R. G.; Benezra, R.; Scheinberg, D. A. Selective Killing of Tumor Neovasculature Paradoxically Improves Chemotherapy Delivery to Tumors. *Cancer Res.* **2010**, *70*, 9277–9286.
10. Jain, R. K. Normalization of Tumor Vasculature: An Emerging Concept in Antiangiogenic Therapy. *Science* **2005**, *307*, 58–62.
11. Sengupta, S.; Eavarone, D.; Capila, I.; Zhao, G.; Watson, N.; Kiziltepe, T.; Sasisekharan, R. Temporal Targeting of Tumour Cells and Neovasculature with a Nanoscale Delivery System. *Nature* **2005**, *436*, 568–572.
12. Yang, T.; Wang, Y.; Li, Z.; Dai, W.; Yin, J.; Liang, L.; Ying, X.; Zhou, S.; Wang, J.; Zhang, X.; *et al.* Targeted Delivery of a Combination Therapy Consisting of Combretastatin A4 and Low-Dose Doxorubicin Against Tumor Neovasculature. *Nanomedicine* **2012**, *8*, 81–92.
13. Colon Cancer: Stages and Survival Rates. www.coloncancer.about.com/od/stagesandsurvivalrates (accessed January 14, 2014).
14. Bałan, B. J.; Słotwiński, R.; Skopińska-Różewska, E. Role of Angiogenesis and Angiogenic Factors in Colorectal Cancer. *Cent. Eur. J. Immunol.* **2009**, *34*, 254–260.
15. Ahlström, H.; Christofferson, R.; Lörelius, L. E. Vascularization of the Continuous Human Colonic Cancer Cell Line LS 174 T Deposited Subcutaneously in Nude Rats. *APMIS* **1988**, *96*, 701–710.
16. Burdick, M. M.; McCaffery, J. M.; Kim, Y. S.; Bochner, B. S.; Konstantopoulos, K. Colon Carcinoma Cell Glycolipids, Integrins, and Other Glycoproteins Mediate Adhesion to HUVECs Under Flow. *Am. J. Physiol.: Cell Physiol.* **2003**, *284*, C977–987.
17. Ward Ward, S.; Morris, E.; Bansback, N.; Calvert, N.; Crellin, A.; Forman, D.; Larvin, M.; Radstone, D. A Rapid and Systematic Review of the Clinical Effectiveness and Cost-Effectiveness of Gemcitabine for the Treatment of Pancreatic Cancer. *Health Technol. Assess.* **2001**, *5*, 1–70.
18. Wang, H.; Li, M.; Rinehart, J. J.; Zhang, R. Pretreatment with Dexamethasone Increases Antitumor Activity of Carboplatin and Gemcitabine in Mice Bearing Human Cancer Xenografts: *In Vivo* Activity, Pharmacokinetics, and Clinical Implications for Cancer Chemotherapy. *Clin. Cancer Res.* **2004**, *10*, 1633–1644.
19. García-Manteiga, J.; Molina-Arcas, M.; Casado, F. J.; Mazo, A.; Pastor-Anglada, M. Nucleoside Transporter Profiles in Human Pancreatic Cancer Cells: Role of hCNT1 in 2′,2′-Difluorodeoxycytidine-Induced Cytotoxicity. *Clin. Cancer Res.* **2003**, *9*, 5000–5008.
20. Mackey, J. R.; Mani, R. S.; Selner, M.; Mowles, D.; Young, J. D.; Belt, J. A.; Crawford, C. R.; Cass, C. E. Functional Nucleoside Transporters are Required for Gemcitabine Influx and Manifestation of Toxicity in Cancer Cell Lines. *Cancer Res.* **1998**, *58*, 4349–4357.
21. Couvreur, P.; Stella, B.; Reddy, L. H.; Hillaireau, H.; Dubernet, C.; Desmaële, D.; Lepêtre-Mouelhi, S.; Rocco, F.; Dereuddre-Bosquet, N.; Clayette, P.; *et al.* Squalenoyl Nanomedicines as Potential Therapeutics. *Nano Lett.* **2006**, *6*, 2544–2548.
22. Réjiba, S.; Reddy, L. H.; Bigand, C.; Parmentier, C.; Couvreur, P.; Hajri, A. Squalenoyl Gemcitabine Nanomedicine Overcomes the Low Efficacy of Gemcitabine Therapy in Pancreatic Cancer. *Nanomedicine* **2011**, *7*, 841–849.
23. Reddy, L. H.; Marque, P. E.; Dubernet, C.; Mouelhi, S. L.; Desmaële, D.; Couvreur, P. Preclinical Toxicology (Subacute and Acute) and Efficacy of a New Squalenoyl Gemcitabine Anticancer Nanomedicine. *J. Pharmacol. Exp. Ther.* **2008**, *325*, 484–490.
24. Reddy, L. H.; Renoir, J. M.; Marsaud, V.; Lepetre-Mouelhi, S.; Desmaële, D.; Couvreur, P. Anticancer Efficacy of Squalenoyl Gemcitabine Nanomedicine on 60 Human Tumor Cell Panel and on Experimental Tumor. *Mol. Pharmaceutics* **2009**, *6*, 1526–1535.
25. Reddy, L. H.; Khoury, H.; Paci, A.; Deroussent, A.; Ferreira, H.; Dubernet, C.; Declèves, X.; Besnard, M.; Chacun, H.; Lepêtre-Mouelhi, S.; *et al.* Squalenoylation Favorably Modifies the *In Vivo* Pharmacokinetics and Biodistribution of Gemcitabine in Mice. *Drug Metab. Dispos.* **2008**, *36*, 1570–1577.
26. Bildstein, L.; Dubernet, C.; Marsaud, V.; Chacun, H.; Nicolas, V.; Gueutin, C.; Sarasin, A.; Bénech, H.; Lepêtre-Mouelhi, S.; Desmaële, D.; *et al.* Transmembrane Diffusion of Gemcitabine by a Nanoparticulate Squalenoyl Prodrug: An Original Drug Delivery Pathway. *J. Controlled Release* **2010**, *147*, 163–170.
27. Hamze, A.; Giraud, A.; Messaoudi, S.; Provot, O.; Peyrat, J. F.; Bignon, J.; Liu, J. M.; Wdzieczak-Bakala, J.; Thoret, S.; Dubois, J.; *et al.* Synthesis, Biological Evaluation of 1,1-Diarylethylenes as a Novel Class of Antimitotic Agents. *ChemMedChem* **2009**, *4*, 1912–1924.

28. Messaoudi, S.; Tréguier, B.; Hamze, A.; Provot, O.; Peyrat, J. F.; Rodrigo De Losada, J.; Liu, J. M.; Bignon, J.; Wdzieczak-Bakala, J.; Thoret, S.; *et al.* Isocombretastatins A *versus* Combretastatins A: The Forgotten isoCA-4 Isomer as a Highly Promising Cytotoxic and Antitubulin Agent. *J. Med. Chem.* **2009**, *52*, 4538–4542.
29. Cushman, M.; Nagarathnam, D.; Gopal, D.; He, H.-M.; Lin, C. M.; Hamel, E. Synthesis and Evaluation of Analogues of (*Z*)-1-(4-Methoxyphenyl)-2-(3,4,5-Trimethoxyphenyl)Ethene as Potential Cytotoxic and Antimitotic Agents. *J. Med. Chem.* **1992**, *35*, 2293–2306.
30. Couvreur, P.; Reddy, L. H.; Mangenot, S.; Poupaert, J. H.; Desmaële, D.; Lepêtre-Mouelhi, S.; Pili, B.; Bourgaux, C.; Amenitsch, H.; Ollivon, M. Discovery of New Hexagonal Supramolecular Nanostructures Formed by Squalenoylation of an Anticancer Nucleoside Analogue. *Small* **2008**, *4*, 247–253.
31. Grant, D. S.; Williams, T. L.; Zahaczewsky, M.; Dicker, A. P. Comparison of Antiangiogenic Activities using Paclitaxel (Taxol) and Docetaxel (Taxotere). *Int. J. Cancer* **2003**, *104*, 121–129.
32. Scholzen, T.; Gerdes, J. The Ki-67 Protein: from the Known and the Unknown. *J. Cell. Physiol.* **2000**, *182*, 311–322.
33. Nielsen, J. S.; McNagny, K. M. Novel Functions of the CD34 Family. *J. Cell Sci.* **2008**, *121*, 3682–3692.
34. Desmaële, D.; Gref, R.; Couvreur, P. Squalenoylation: A Generic Platform for Nanoparticular Drug Delivery. *J. Controlled Release* **2012**, *161*, 609–618.
35. Bildstein, L.; Pili, V.; Marsaud, V.; Wack, S.; Meneau, F.; Lepêtre-Mouelhi, S.; Desmaële, D.; Bourgaux, C.; Couvreur, P.; Dubernet, C. Interaction of an Amphiphilic Squalenoyl Prodrug of Gemcitabine with Cellular Membranes. *Eur. J. Pharm. Biopharm.* **2011**, *79*, 612–620.
36. Giavazzi, R.; Jessup, J. M.; Campbell, D. E.; Walker, S. M.; Fidler, I. J. Experimental Nude Mouse Model of Human Colorectal Cancer Liver Metastases. *JNCI, J. Natl. Cancer Inst.* **1986**, *77*, 1303–1308.
37. Spiga, S.; Acquas, E.; Puddu, M. C.; Mulas, G.; Lintas, A.; Diana, M. Simultaneous Golgi-Cox and Immunofluorescence Using Confocal Microscopy. *Brain Struct. Funct.* **2011**, *216*, 171–182.